Molecular characterization of perivascular drainage pathways in the murine brain

Melanie-Jane Hannocks[1,2], Michelle E Pizzo[3,4], Jula Huppert[1,2], Tushar Despande[1,2], N. Joan Abbott[5], Robert G Thorne[3,4,6,7] and Lydia Sorokin[1,2]

[1]Institute of Physiological Chemistry and Pathobiochemistry and [2]Cells-in-Motion Cluster of Excellence, University of Muenster, 48149 Muenster, Germany; [3]Pharmaceutical Sciences Division, University of Wisconsin-Madison School of Pharmacy and [4]Clinical Neuroengineering Training Program, University of Wisconsin-Madison, Madison, Wisconsin 53705, United States; [5]Institute of Pharmaceutical Science, King's College, London SE1 9NH, UK; [6]Neuroscience Training Program & Center for Neuroscience, and [7]Cellular and Molecular Pathology Graduate Training Program, University of Wisconsin-Madison, Madison, Wisconsin 53705, United States.

Corresponding author:

Lydia Sorokin

Institute of Physiological Chemistry and Pathobiochemistry

University of Muenster, Waldeyerstrasse 15, 48149 Muenster, Germany

Tel +49 251 8355581; fax +49 251 83 55596; email: sorokin@uni-muenster.de

Material and Methods

Immunofluorescence microscopy (long protocol)

Sections (100 µm) were treated with 1% bovine serum albumin (BSA)/0.5% TritonX-100 in PBS for 8 hours before being incubated for two nights at 4°C with primary antibodies (laminin α1 and laminin α2, Supplementary Table 1). Bound antibodies were visualized using Alexa 488-conjugated goat anti-rat and Alexa 647-conjugated goat anti-rabbit secondary antibodies (Dianova and Molecular Probes) diluted in PBS containing 1µg/ml DAPI (Molecular Probes, Germany) and 0.5% Triton X-100 after overnight incubation at 4°C. Sections were examined and documented using a LSM 700 confocal microscope (Zeiss, Germany). Images were analysed using Volocity 6.3 software (PerkinElmer, USA). These stainings were repeated twice on two different mice.

Supplementary Table 1. Primary Antibodies Employed in Immunofluorescence Analyses of Vascular Basement Membrane and Cellular Proteins

Target Molecule	Antibody Designation/Clone	Reference/Source
Laminin α1	rabbit anti-mouse/317*	[1]
	rat anti-mouse/200	[2]
Laminin α2	rabbit anti-mouse/401*	[3]
	rat anti-mouse/4H8-2	[3, 4]
Laminin α4	rabbit anti-mouse/377	[3]
Laminin α5	rabbit anti-mouse/405*	[3]
	rat anti-mouse/4G6	[5]
Laminin γ1	rat anti-mouse/3E10	[6, 7]
	mouse anti-human/D18*	[8]
SMA	Cy3 mouse anti-mouse/1A4	Sigma, Germany, C6198
Collagen I	rabbit anti-mouse	Chemicon, Germany, AB 756P
Collagen III	goat anti-mouse	SouthernBiotech, Germany, 1330-01
ERTR7	rat anti-mouse/ER-TR7	Dianova, Germany, T2109
Plectin	guinea pig anti-human	Progen, Germany, GP21
E-Cadherin/Uvomorulin	rabbit anti-mouse uvomorulin	[9]
	rat anti-mouse/DECMA-1	Sigma, Germany, U3254
GFAP	Cy3 mouse anti-pig/G-A-5	Sigma, Germany, C9205
	Alexa Fluor 488 mouse anti-pig/G-A-5	eBioscience, Germany, 53-9892
AQP4	rabbit anti-rat	Millipore, Germany, AB3954
F4/80	Rat anti-mouse/A3-1	Serotec, Germany, MCA497G
Iba-1	Rabbit anti-mouse*	Wako, Germany, 019-19741

* Functional in rat tissues

References

1. Durbeej M, Fecker L, Hjalt T, et al. Expression of laminin alpha 1, alpha 5 and beta 2 chains during embryogenesis of the kidney and vasculature. *Matrix Biol*. 1996; 15: 397-413.
2. Sorokin LM, Conzelmann S, Ekblom P, Aumailley M, Battaglia C and Timpl R. Monoclonal antibodies against laminin A chain fragment E3 and their effects on cell- and heparin-binding, and on kidney development. *Exp Cell Res*. 1992; 201: 137-44.
3. Ringelmann B, Roder C, Hallmann R, et al. Expression of laminin alpha1, alpha2, alpha4, and alpha5 chains, fibronectin, and tenascin-C in skeletal muscle of dystrophic 129ReJ dy/dy mice. *Exp Cell Res*. 1999; 246: 165-82.
4. Schuler F and Sorokin LM. Expression of laminin isoforms in mouse myogenic cells in vitro and in vivo. *J Cell Sci*. 1995; 108: 3795-805.
5. Sorokin LM, Pausch F, Frieser M, Kroger S, Ohage E and Deutzmann R. Developmental regulation of the laminin alpha5 chain suggests a role in epithelial and endothelial cell maturation. *Dev Biol*. 1997; 189: 285-300.
6. Sixt M, Hallmann R, Wendler O, Scharffetter-Kochanek K and Sorokin LM. Cell adhesion and migration properties of b2-integrin negative, polymorphonuclear granulocytes (PMN) on defined extracellular matrix molecules: relevance for leukocyte extravasation. *J Biol Chem*. 2001; 276: 18878-87.
7. Sixt M, Kanazawa N, Selg M, et al. The conduit system transports soluble antigens from the afferent lymph to resident dendritic cells in the T cell area of the lymph node. *Immunity*. 2005; 22: 19-29.
8. Engvall E, Earwicker D, Haaparanta T, Ruoslahti E and Sanes JR. Distribution and isolation of four laminin variants: tissue restricted distibution of heterotrimers assembled from five different subunits. *Cell Regul*. 1990; 1: 731-40.
9. Boller K, Vestweber D and Kemler R. Cell-adhesion molecule uvomorulin is localized in the intermediate junctions of adult intestinal epithelial cells. *J Cell Biol*. 1985; 100: 327-32.

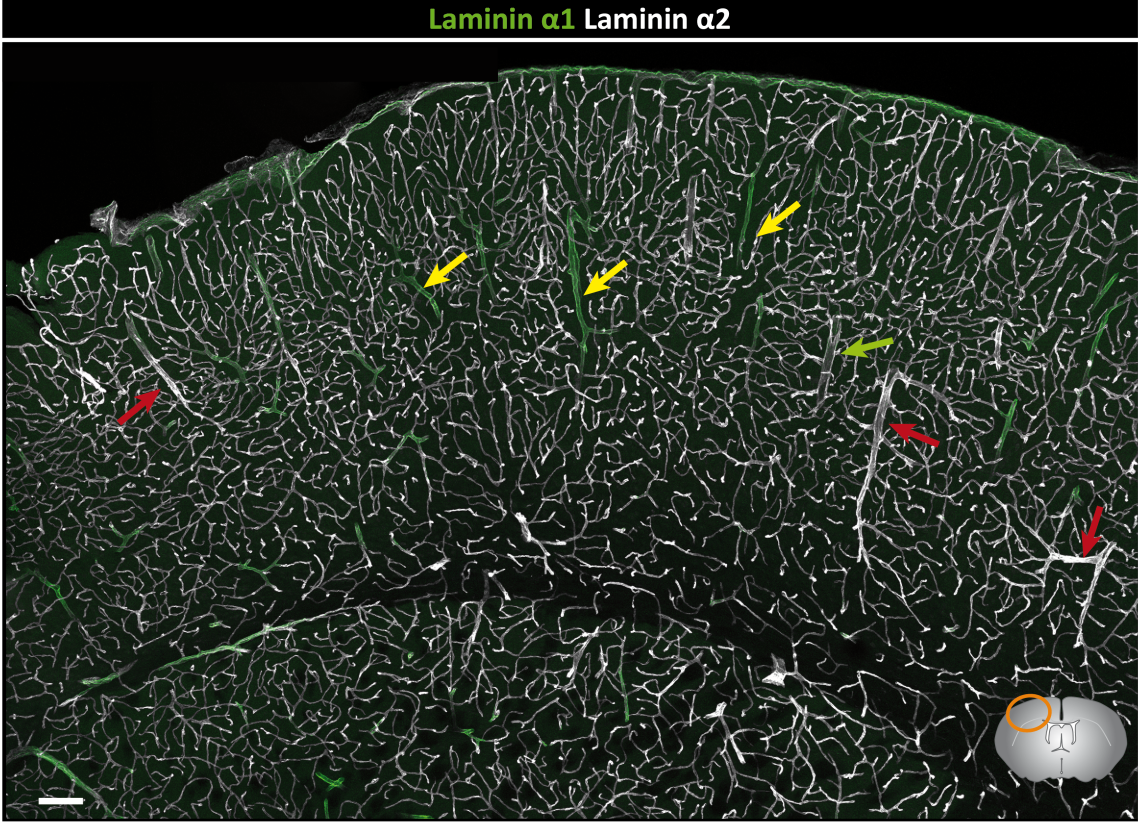

Supplemental Figure 1. Basement membrane laminin α1 and α2 staining patterns
Adult mouse brain tissue sections (100 μm) were immunofluorescently stained for the BM proteins laminin α1 and laminin α2. Using longer antibody incubation times (two nights with primary antibody and one night with secondary antibody) revealed that a small number of venules were double positive for laminin α1 and α2 (green arrow) in addition to the laminin $\alpha1^{+}$/laminin $\alpha2^{low}$ arterioles (yellow arrows) and the laminin $\alpha1^{-}$/laminin $\alpha2^{high}$ venules (red arrows) that were detected with the shorter incubation protocol (overnight with primary antibody and 2 hours with secondary antibody). The diagram in the lower right hand corner shows the location of the image. Images shown represent studies performed on two mice.

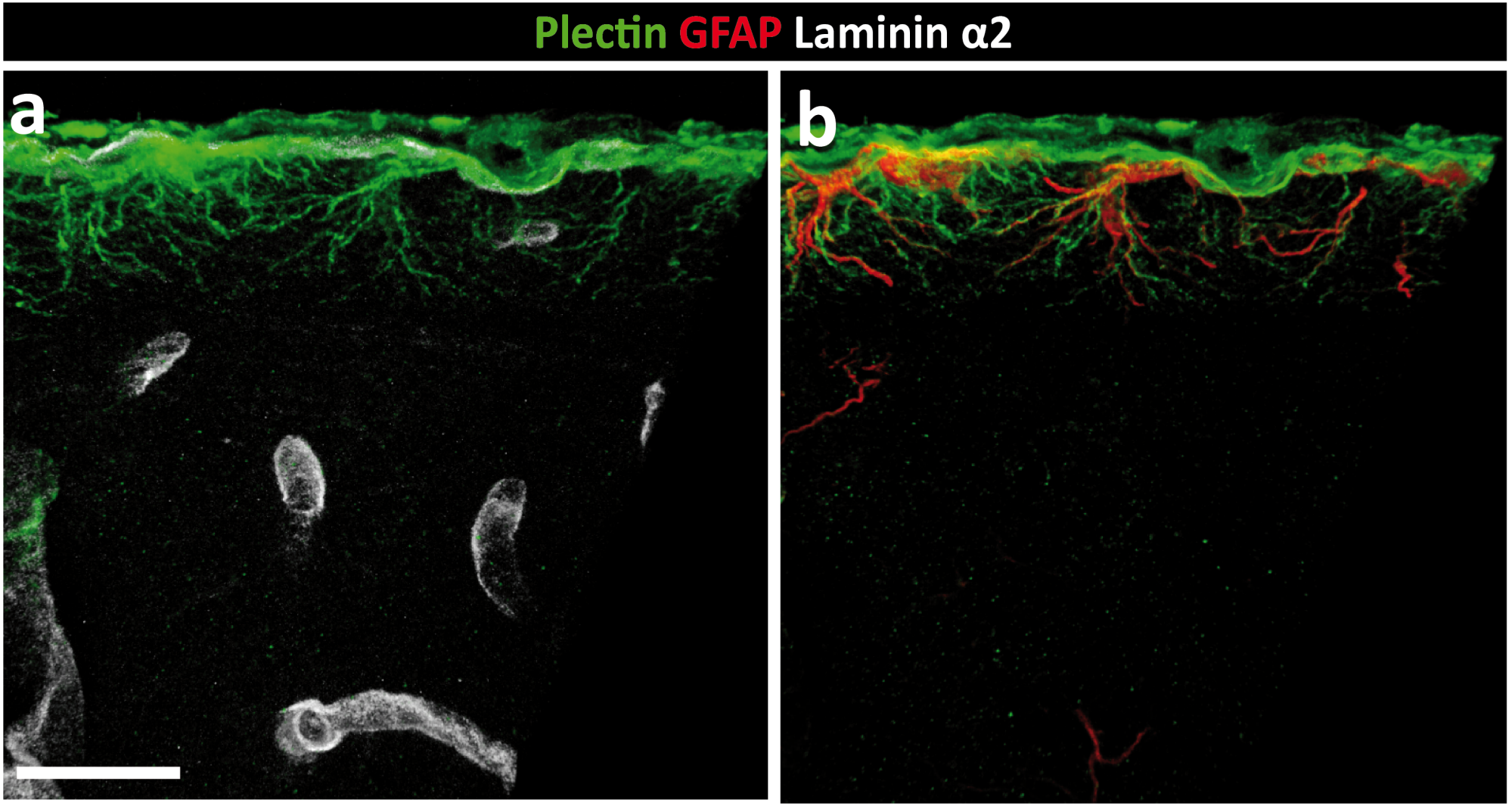

Supplemental Figure 2. Expression of plectin by the glia limitans

Adult mouse brain tissue sections (100 µm) were immunofluorescently stained for the epithelial cell marker plectin, basement membrane laminin α2, and glial fibrillary acidic protein (GFAP). (a) Intense plectin staining was seen at the surface of the brain and along a few laminin a^+ vessels in the cortex. (b) Intense plectin staining at the surface of the brain colocalised with a subpopulation of $GFAP^+$ astroglia in addition to the epithelial cells of the pial and arachnoid layer. Images shown represent studies performed on eight mice. Scale bar: 20 µm

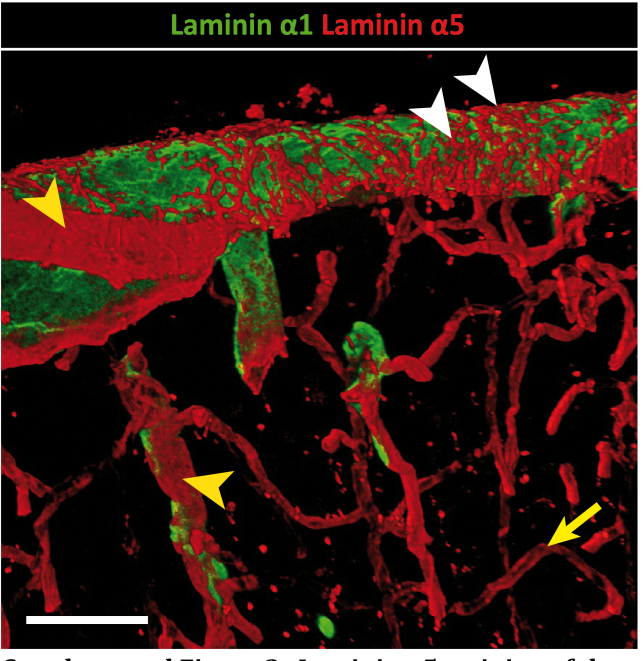

Supplemental Figure 3. Laminin α5 staining of the arachnoid basement membrane (BM)
Adult mouse brain tissue sections (100 μm) were immunofluorescently stained for the BM proteins laminin α5 and laminin α1. The arachnoid BM appeared filigree with areas of high (white arrow heads) and low laminin α5 staining. In contrast, the pial epithelial BM showed continuous laminin α1 staining. Endothelial BMs (yellow arrow) and smooth muscle BMs (yellow arrow head) are also positive for laminin α5. Images shown represent studies performed on eight mice. Scale bar: 50 μm

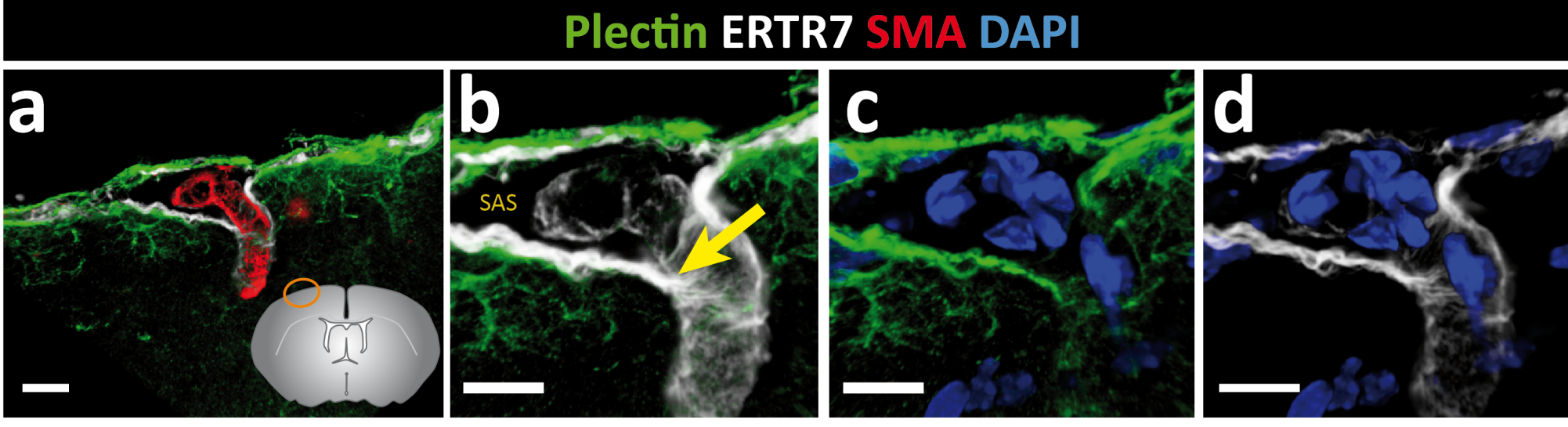

Supplemental Figure 4. Leptomeningeal fibroblasts associate with subarachnoid arteries.

Adult mouse brain tissue sections (100 µm) were immunofluorescently stained to determine the relationship between the inner plectin$^+$ pial layer, ERTR7$^+$ leptomeningial cells and SMA$^+$ arteries in the subarachnoid space. (a,b) ERTR7$^+$ cells lining the surface of the brain fuse with leptomeningial ERTR7$^+$ fibroblasts around arteries in the subarachnoid space (SAS) as they penetrate into the parenchyma (yellow arrow in (b)). The plectin$^+$ layer is restricted to the brain surface and penetrating arterioles and is not associated with arteries in the SAS. Single stainings for plectin and ERTR7 are shown in (c) and (d) respectively. DAPI marks nuclei. The diagram in (a) shows the location of the image. Images shown represent studies performed on eight mice. Scale bar: (a-d) 15 µm.

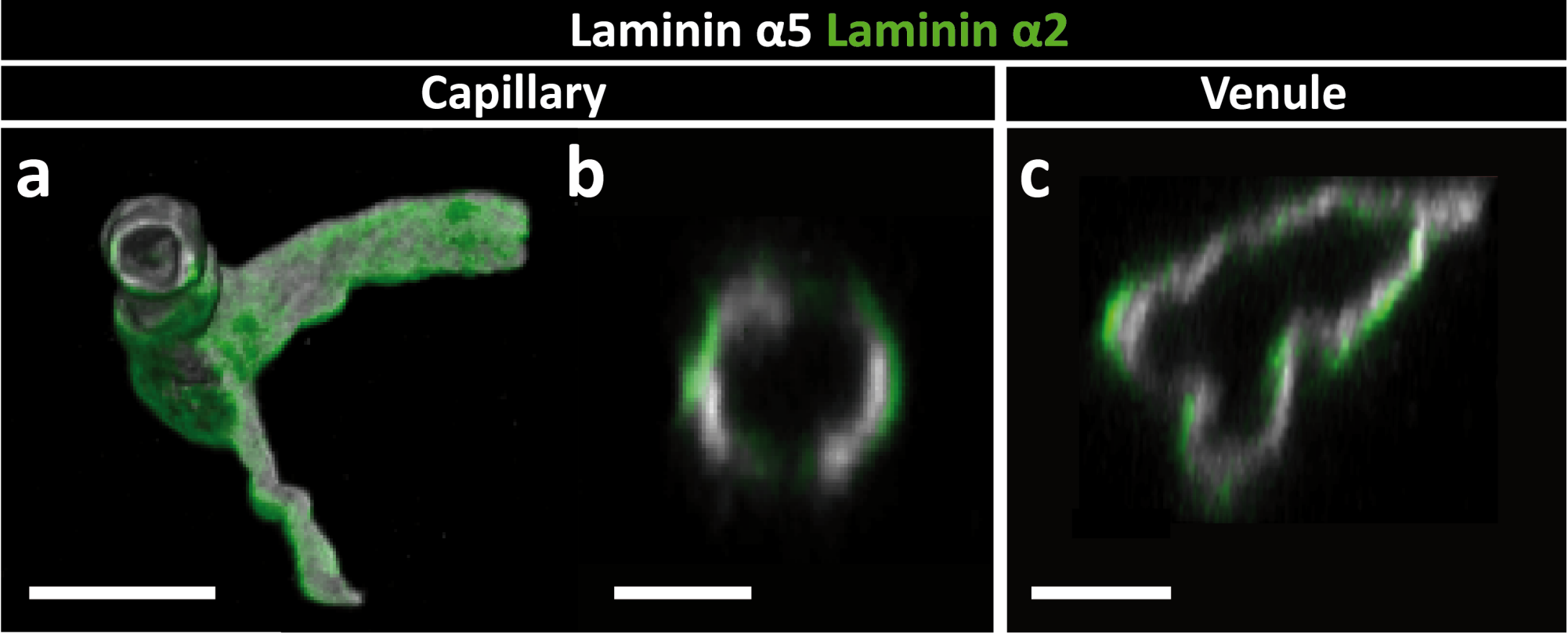

Supplemental Figure 5. Potential perivascular pathways from arterioles through to capillaries and veins

Adult mouse brain tissue sections (100 μm) were immunofluorescently stained for the BM proteins laminin α5 and laminin α2. A distinct orientation of the laminin $\alpha2^{+}$ parenchymal BM to the laminin $\alpha5^{+}$ endothelial BM was noted from the capillary bed (a, b) through to the venules (c). Vessels depicted are from the parenchyma of the dorsal cortex. Images shown represent studies performed on three mice.
Scale bars: (a, c) 10 μm, (b) 5 μm.

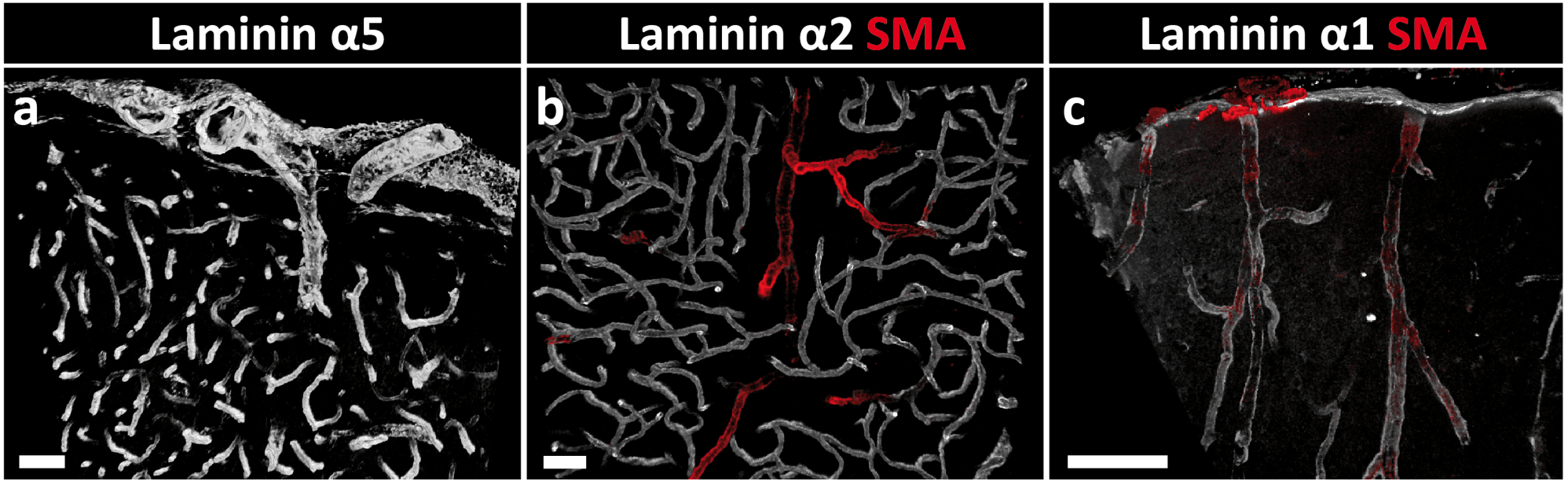

Supplemental Figure 6. Basement membrane laminin α-chain localization in rat brains

Adult rat brain tissue sections (100 µm) were immunofluorescently stained for the BM proteins laminin α5 (a), laminin α2 (b) and laminin α1 (c) and SMA. All three laminin BM proteins showed similar distribution patterns as identified in mouse tissue. Images shown represent studies performed on three rats.

Scale bars: (a, b) 50 µm, (c) 50 µm

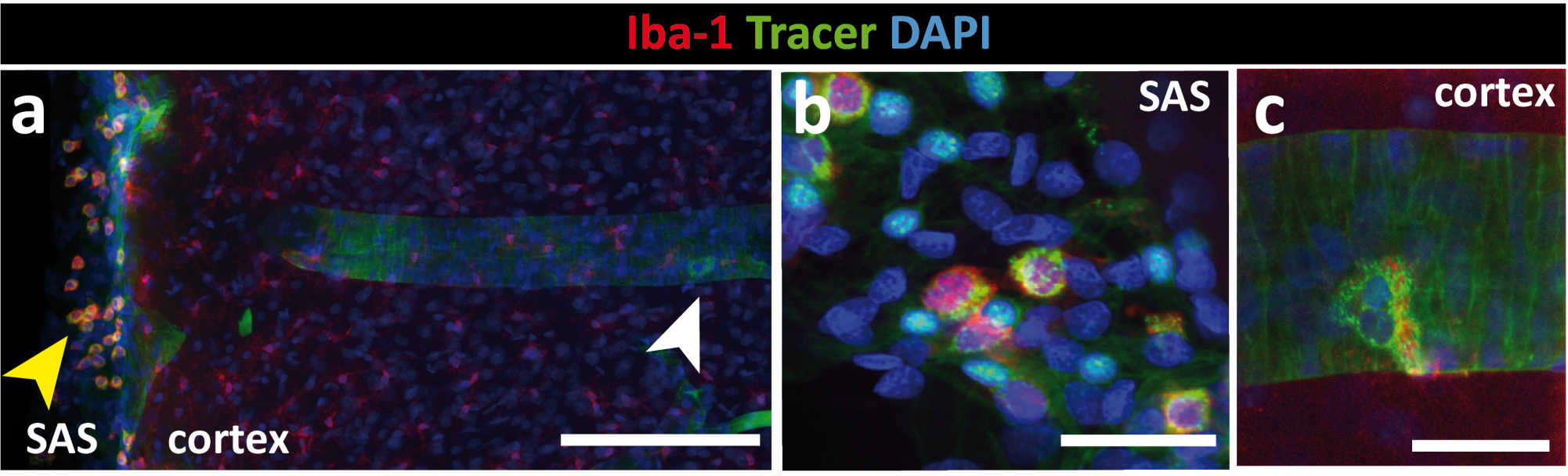

Supplemental Figure 7. Macrophages phagocytose intracisternally infused tracer

Tracer (goat anti-rabbit IgG-Alexa Fluor 488) was infused into the CSF of adult rats via the cisterna magna. 100µm tissue sections were immunofluorescently stained for Iba-1. (a) Colocalization of tracer with Iba-1$^+$ macrophages in the subarachnoid space (yellow arrowhead) and perivascular compartments (white arrowhead) was observed. DAPI marks nuclei. Higher magnification of meningeal macrophages in the subarachnoid space and perivascular macrophages are shown in (b) and (c), respectively. Images shown represent studies performed on three rats.

Scale bar: (a) 150 µm, (b, c) 25µm